Search for Higgs boson pair production in $bb\gamma\gamma$ final state in pp collisions at $\sqrt{s}$ = 13 TeV with the ATLAS detector

Zihang Jia[1,2]

[1]*IHEP*, [2]*Nanjing University*

Motivation – Higgs self-coupling

- **The Higgs boson** completes the **Standard Model** of Particle Physics.
- However, the shape of **the Higgs potential** has yet to be measured.
- We can probe **the Higgs potential** by measuring the **Higgs self-coupling (λ)**.

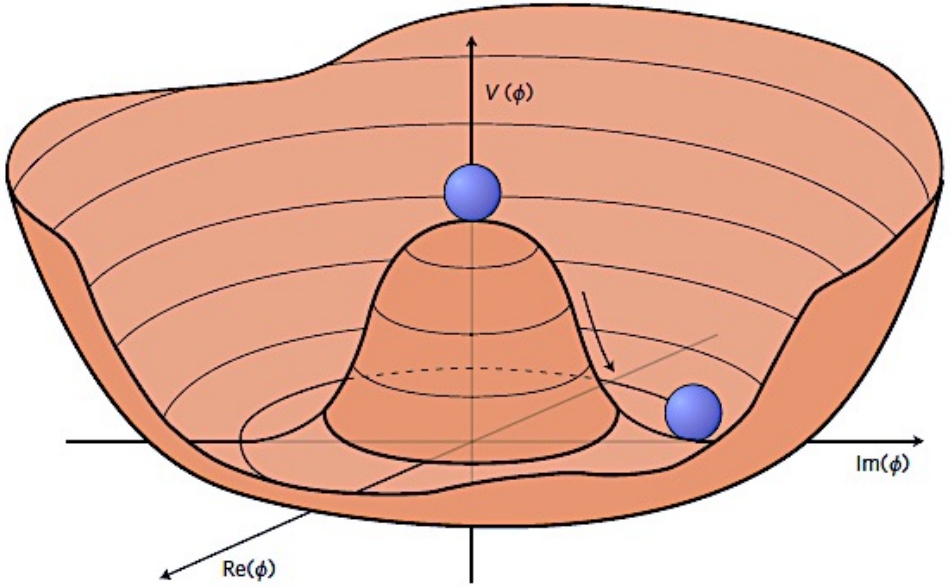

$$V(h) \simeq \frac{1}{2}m_H^2 h^2 + \lambda v h^3 + \frac{1}{4}\lambda h^4 + \ldots$$

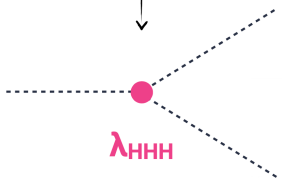

$$\kappa_\lambda = \frac{\lambda_{HHH}}{\lambda_{HHH}^{SM}}$$

Measuring **HH production** gives us access to the **trilinear** Higgs self−coupling (λ_{HHH})

HH production at LHC

SM

Gluon-gluon fusion (ggFHH)

Destructive interference, 1000x smaller than single H production

- σNNLO = **31.05** [fb] @13 TeV, mH = 125 GeV

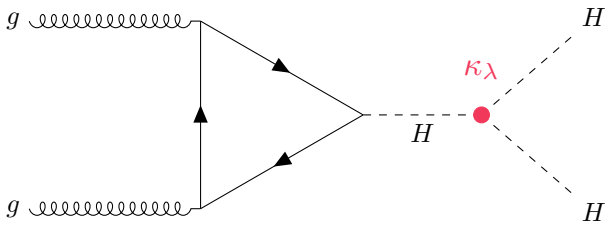

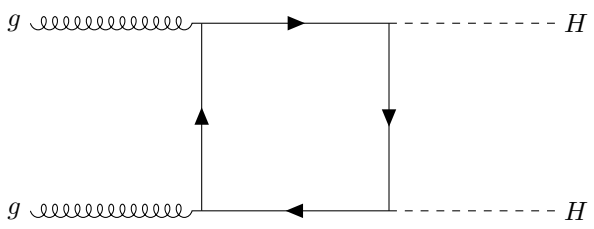

Vector boson fusion (VBFHH)

- σN3LO = **1.726** [fb] @13 TeV, mH = 125 GeV

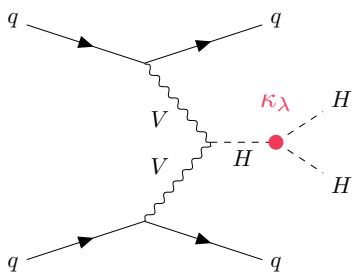

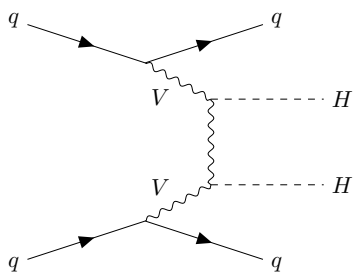

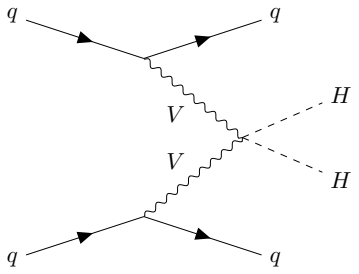

BSM enhancement

Non-resonant HH production

- Anomalous couplings ($\kappa_\lambda \neq 1$, etc.)

$$\kappa_\lambda = \frac{\lambda_{HHH}}{\lambda_{HHH}^{SM}}$$

Resonant HH production

- X: a narrow-width scalar particle

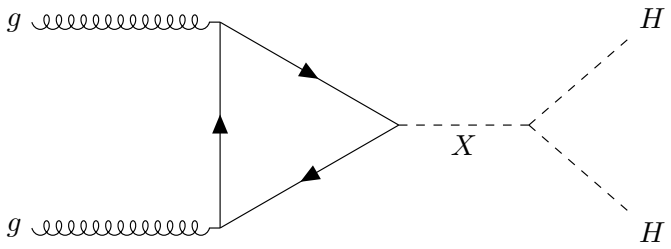

HH$\gamma\gamma bb$ Analysis overview

Search for **Non-resonant** and **Resonant** HH production in $\boldsymbol{bb\gamma\gamma}$ **channel** (full Run2 data, 139 fb^{-1}).

One of the most sensitive HH final states:

- $H \to bb$: largest branching ratio
- $H \to \gamma\gamma$: excellent photon resolution, clean final state

	bb	WW	ττ	ZZ	γγ
bb	34%				
WW	25%	4.6%			
ττ	7.3%	2.7%	0.39%		
ZZ	3.1%	1.1%	0.33%	0.069%	
γγ	0.26%	0.10%	0.028%	0.012%	0.0005%

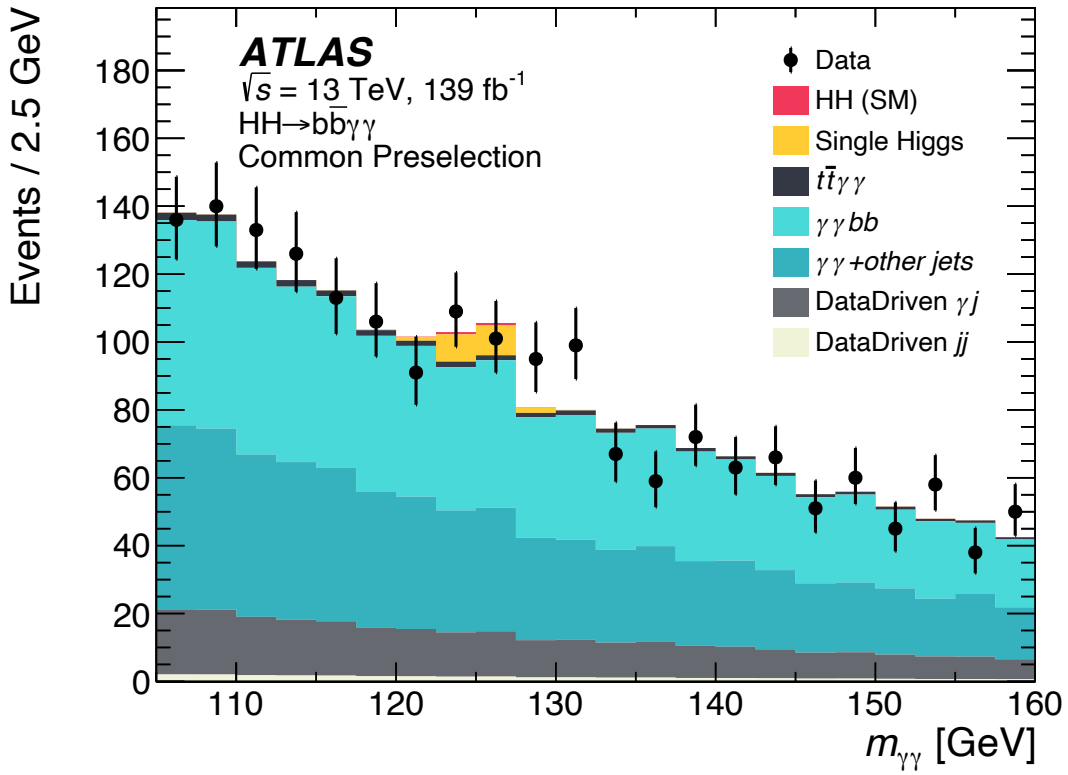

HH$\gamma\gamma bb$ Analysis overview

Search for **Non-resonant** and **Resonant** HH production in $\boldsymbol{\gamma\gamma bb}$ **channel** (full Run2 data, 139 fb^{-1}).

Main backgrounds

- Single Higgs production $\mathrm{H} \rightarrow \gamma\gamma$
- Non-resonant $\gamma\gamma$+jets backgrounds

Common Preselection

- 2 identified and isolated photons
- 2 b-tagged jets (77% DL1r b-tagging efficiency)
- < 6 central jets (reject $\boldsymbol{t\bar{t}H}$ hadronic decay)
- 0 leptons (reject $\boldsymbol{t\bar{t}H}$ leptonic decay)

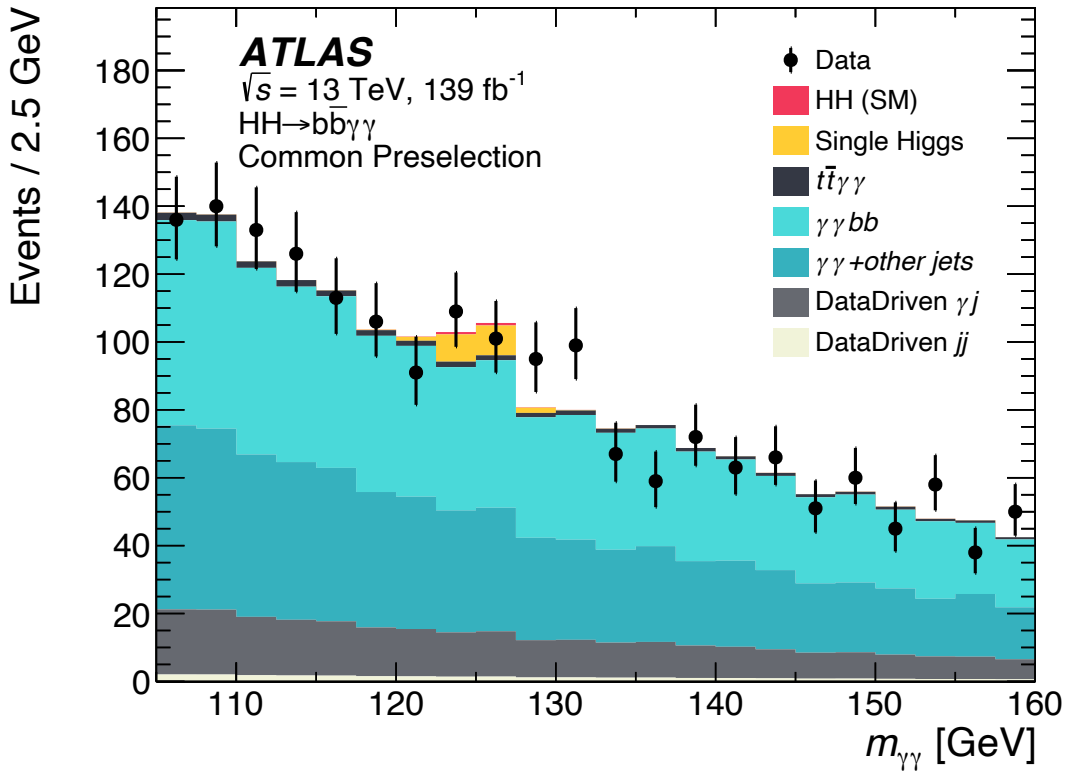

Multivariate method designed to reject background processes.

Statistical results obtained from **a fit of $\boldsymbol{m_{\gamma\gamma}}$ distribution.**

Event categorization

Both **Non-resonant** and **Resonant** search rely on a combination of ($m^*_{\gamma\gamma bb}$ + BDT score).

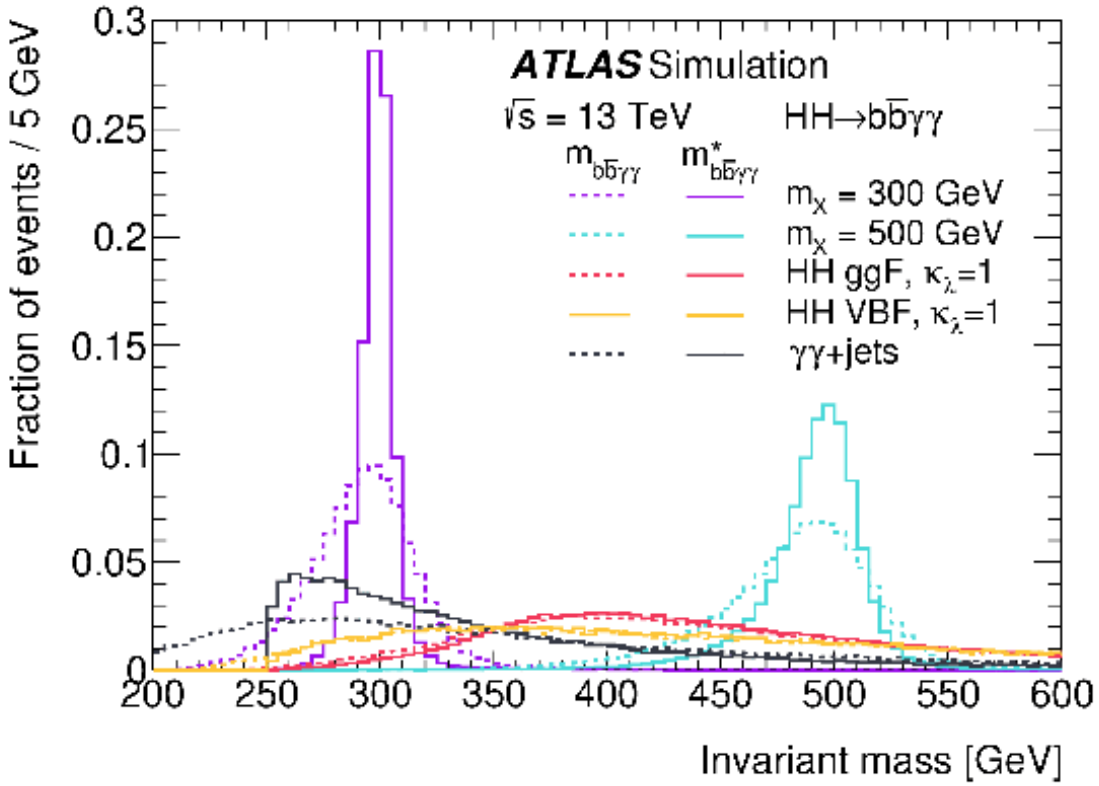

Modified invariant mass

$$m^*_{\gamma\gamma bb} = m_{\gamma\gamma bb} - m_{\gamma\gamma} - m_{bb} + 250\ GeV$$

Provide cancellation of experimental **resolution** effects

- ➢ particularly for the resonant signals

Event categorization

Non-resonant analysis: target SM HH → $\gamma\gamma bb$ processes, and possible modifications to κ_λ.

➢ Two $m^*_{\gamma\gamma bb}$ mass regions

- Provide enhanced sensitivity to $\boldsymbol{\kappa_\lambda}$

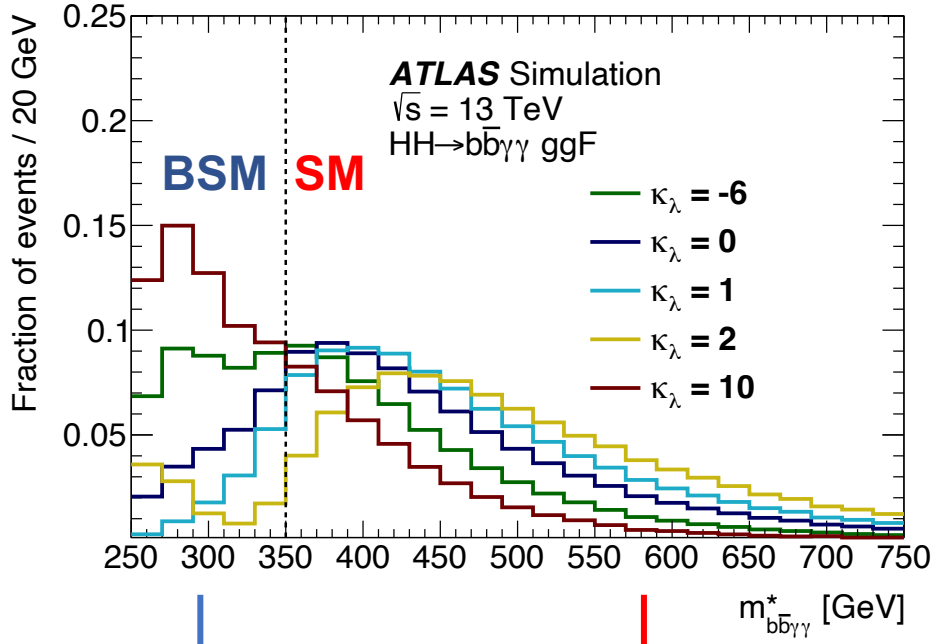

$m^*_{\gamma\gamma bb} < 350\ GeV$
Low mass region
Target κ_λ=10

$m^*_{\gamma\gamma bb} \geq 350\ GeV$
High mass region
Target κ_λ=1

➢ Boosted Decision Tree, one BDT in each mass region

- Against diphoton continuum and single Higgs backgrounds
- Input variables: photon, jet and missing transverse energy variables

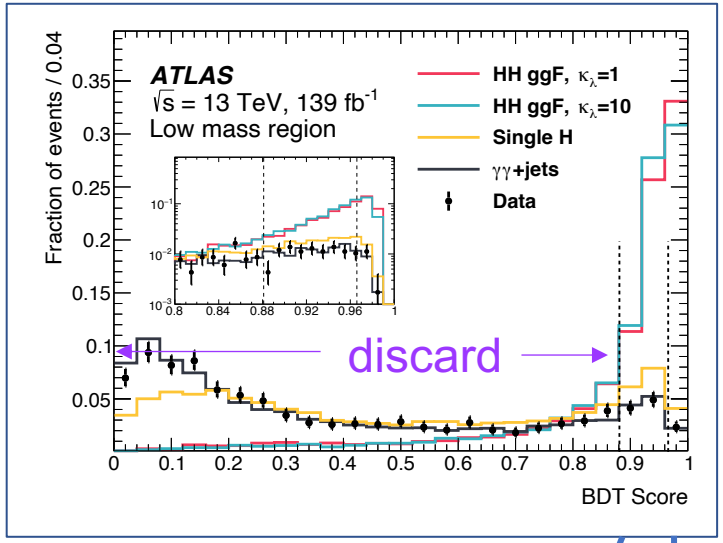

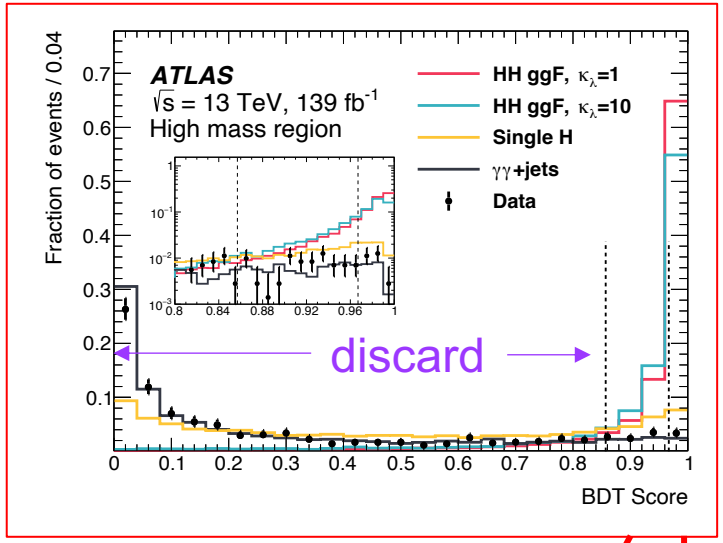

Loose Tight **Loose Tight**

Boundaries chosen to maximize combined expected significance

Event categorization

Resonant analysis: target $X \rightarrow HH \rightarrow \gamma\gamma bb$ processes, with $m_X \in [251, 1000]$ GeV.

➢ One mass region for each m_X

- 2σ window cut around each m_X

  σ from a fit to $m^*_{\gamma\gamma bb}$ using Crystal Ball function

  Relaxed to 4σ for m_X = 900, 1000 GeV

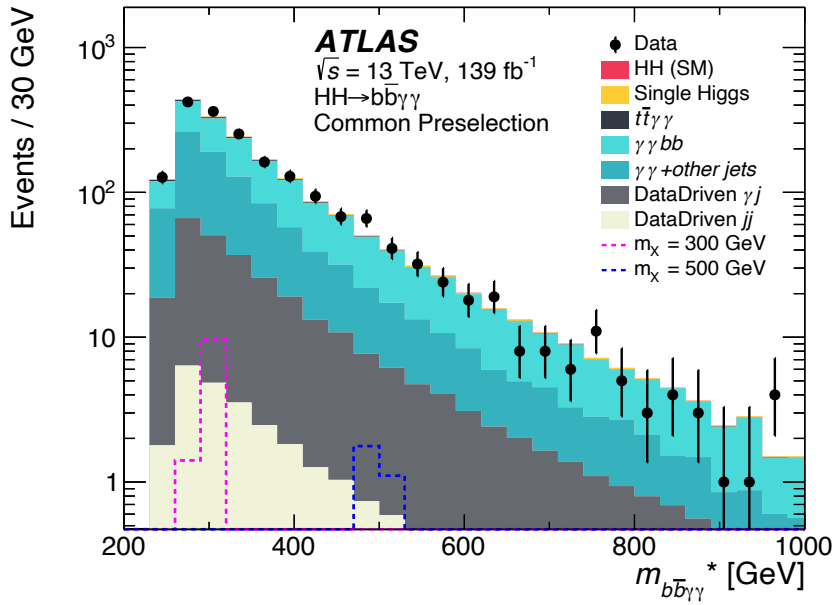

➢ Boosted Decision Tree

- Two separate BDTs against $\gamma\gamma$+$t\bar{t}\gamma\gamma$ and **single Higgs** backgrounds
- Cut on the **combined BDT score** for each m_X
- Input variables: photon, jet and missing transverse energy variables

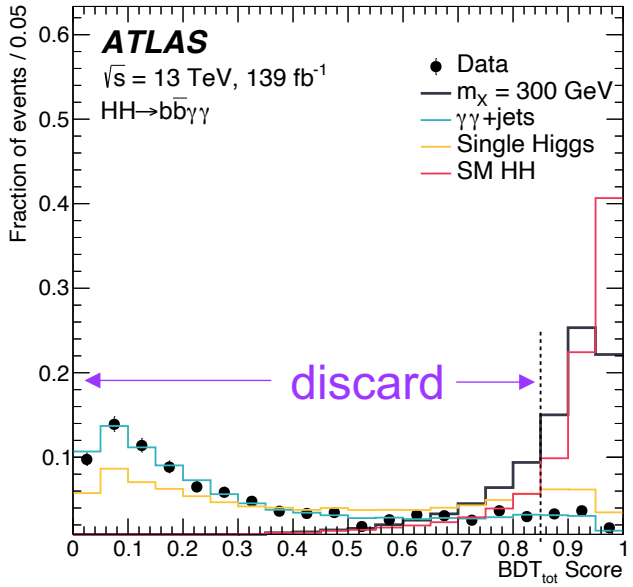

$$\mathrm{BDT_{tot}} = \frac{1}{\sqrt{C_1^2 + C_2^2}} \sqrt{C_1^2 \left(\frac{\mathrm{BDT}_{\gamma\gamma} + 1}{2}\right)^2 + C_2^2 \left(\frac{\mathrm{BDT}_{\mathrm{Single}H} + 1}{2}\right)^2}$$

C_1, C_2 and the BDT_{tot} cut value are **scanned** to maximize the significance

Signal and background modeling

- **Signal parameterization - Double sided crystal ball (DSCB) function**

  Non-resonant analysis

  - Fit to SM $\boldsymbol{HH}$ signal MC, model shared with $\boldsymbol{H}$ background
  - No sizable dependence on κ_λ is observed

  Resonant analysis

  - Fit to resonance signal MC, model shared with SM $\boldsymbol{HH}$ and $\boldsymbol{H}$ background

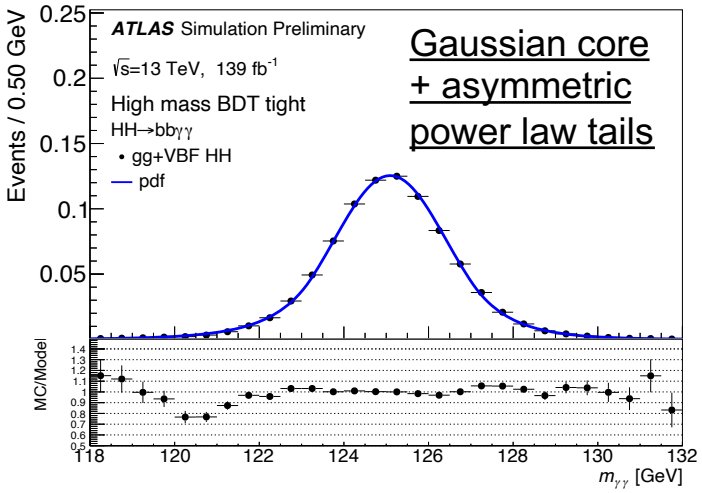

- **Continuum background parameterization - Exponential function**

  - Function form determined from **spurious signal** study
  - **Spurious signal** = a bias estimated from a **S+B** fit to a **B-only** MC template

    also a systematic uncertainty assigned to the function **choice**
  - Functions with smaller **spurious signal** are preferred

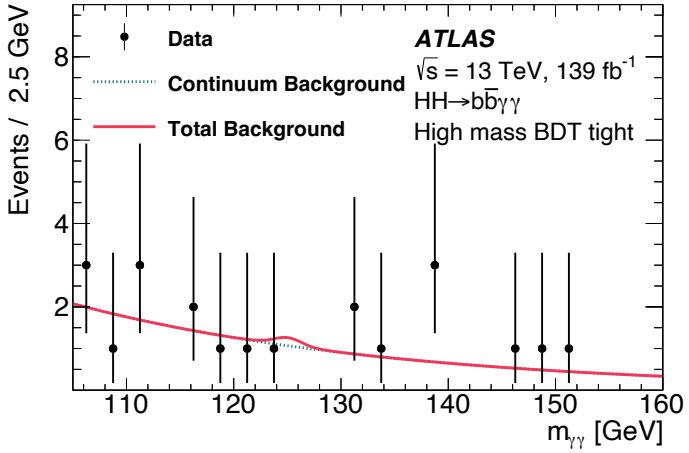

Statistical results obtained from a **maximum-likelihood fit** to the $\boldsymbol{m_{\gamma\gamma}}$ distribution

Results

No signal is observed. **Exclusion limits at 95%CL** are set.

Non-resonant

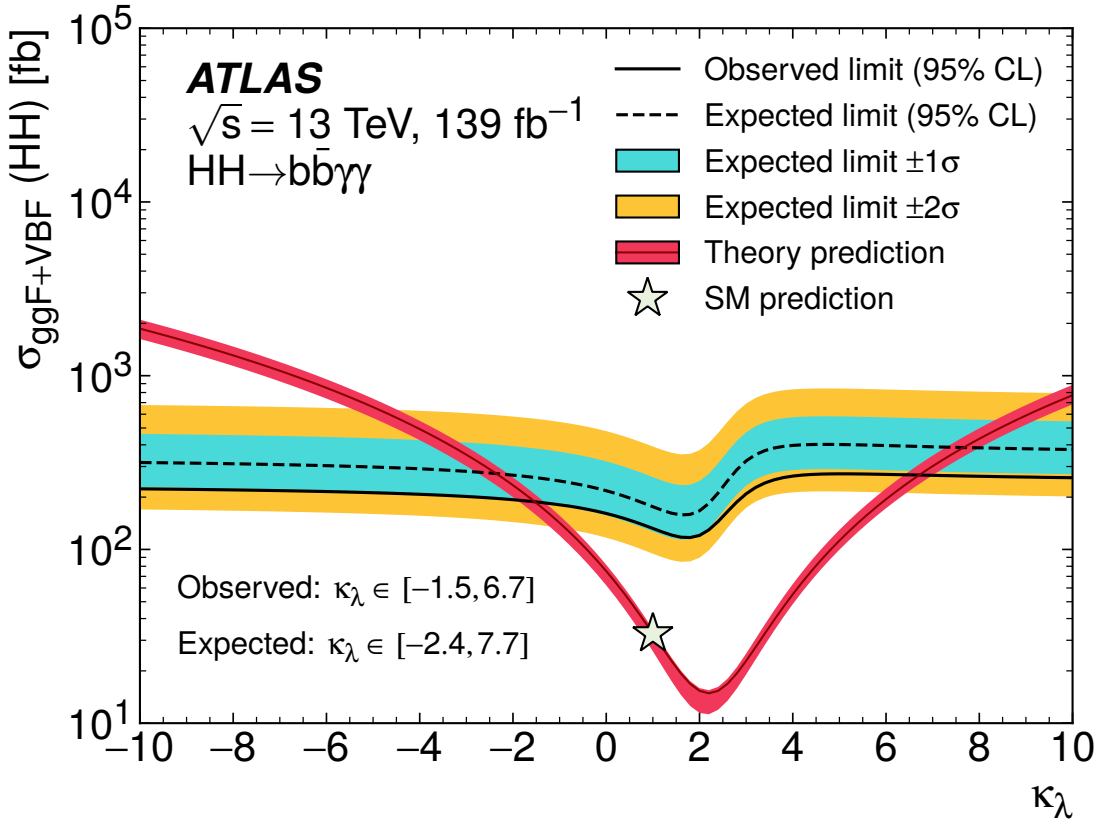

	Upper limit on $\sigma(HH)$	κ_λ constraint
Observed	4.2 x SM	[−1.5, 6.7]
(Expected)	5.7 x SM	[−2.4, 7.7]

ATLAS 36 fb^{-1} JHEP 11 (2018) 040

$\sigma(HH)$ **limit:** 22 (28) x SM — Improved by a factor of 5

κ_λ **constraint:** [-8.2, 13.2] ([-8.3, 13.2]) — Shrinks by a factor of ~2

CMS JHEP 03 (2021) 257

$\sigma(HH)$ **limit:** 7.7 (5.2) x SM

κ_λ **constraint:** [-3.3, 8.5] ([-2.5, 8.2])

Results

No signal is observed. **Exclusion limits at 95%CL** are set.

Resonant

$\boldsymbol{\sigma}(\mathbf{X} \rightarrow \mathbf{HH})$ **upper limits** vary between 610 fb and 47 fb (360 fb and 43 fb) in $m_X \in [251, 1000]$ GeV

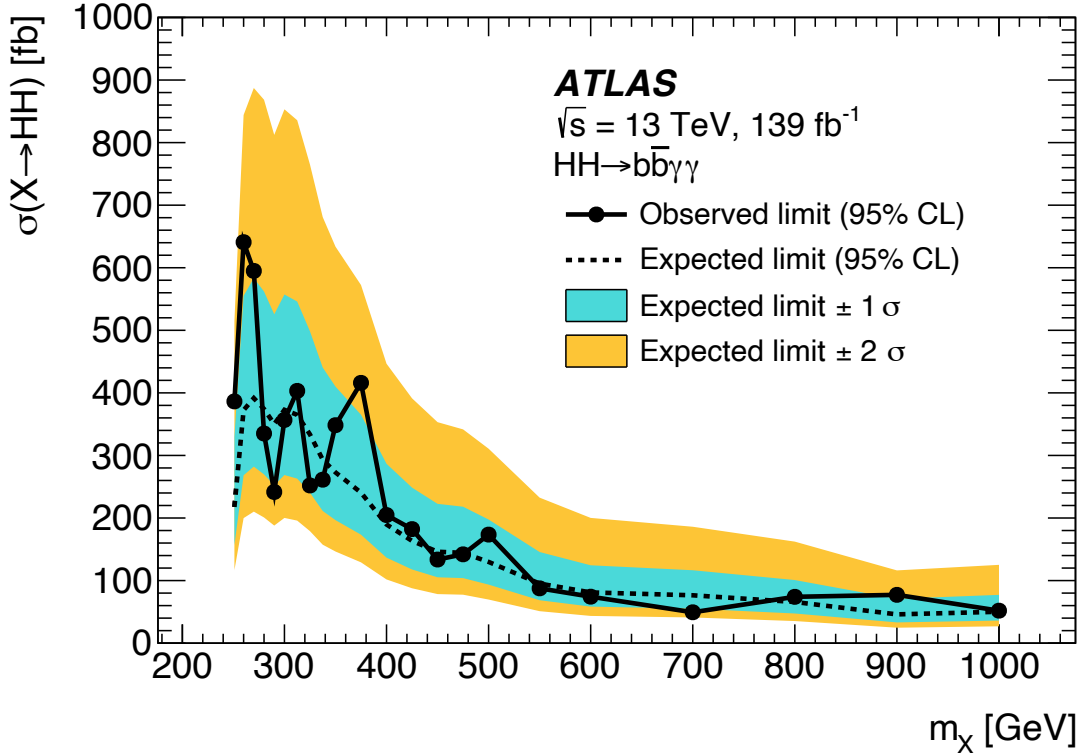

ATLAS 36 fb^{-1} JHEP 11 (2018) 040

$\boldsymbol{\sigma}(\mathbf{X} \rightarrow \mathbf{HH})$ upper limits vary between 1.1 pb and 0.12 pb (0.9 pb and 0.15 pb) in $m_X \in [260, 1000]$ GeV

Improved by a factor of 2-3 depending on the m_X value.

The analyzed mass range expanded to **lower values**.

Summary

Searches for **non-resonant** and **resonant** HH production are performed in the $bb\gamma\gamma$ final state (139 fb^{-1}).

No significant excess with respect to the SM background expectation is observed.

Upper limits on $\boldsymbol{\sigma(HH)}$ and constraints on $\boldsymbol{\kappa_\lambda}$ are set.

Improvement compared to the previous ATLAS result based on 36 fb^{-1} data:

- Extended **data set** by a factor of ~4
- **Categorization** based on $m^*_{\gamma\gamma bb}$ and **multivariate** event selections
- More precise **object reconstruction and calibration**

Publication: PhysRevD.106.052001

中国科学院高能物理研究所
Institute of High Energy Physics
Chinese Academy of Sciences

NANJING UNIVERSITY 1902

ATLAS EXPERIMENT

Thanks!

JHEP 11 (2018) 040 (ATLAS 36 fb^{-1})

JHEP 03 (2021) 257 (CMS)

ATLAS-PHYS-PUB-2021-031 (HH summary)

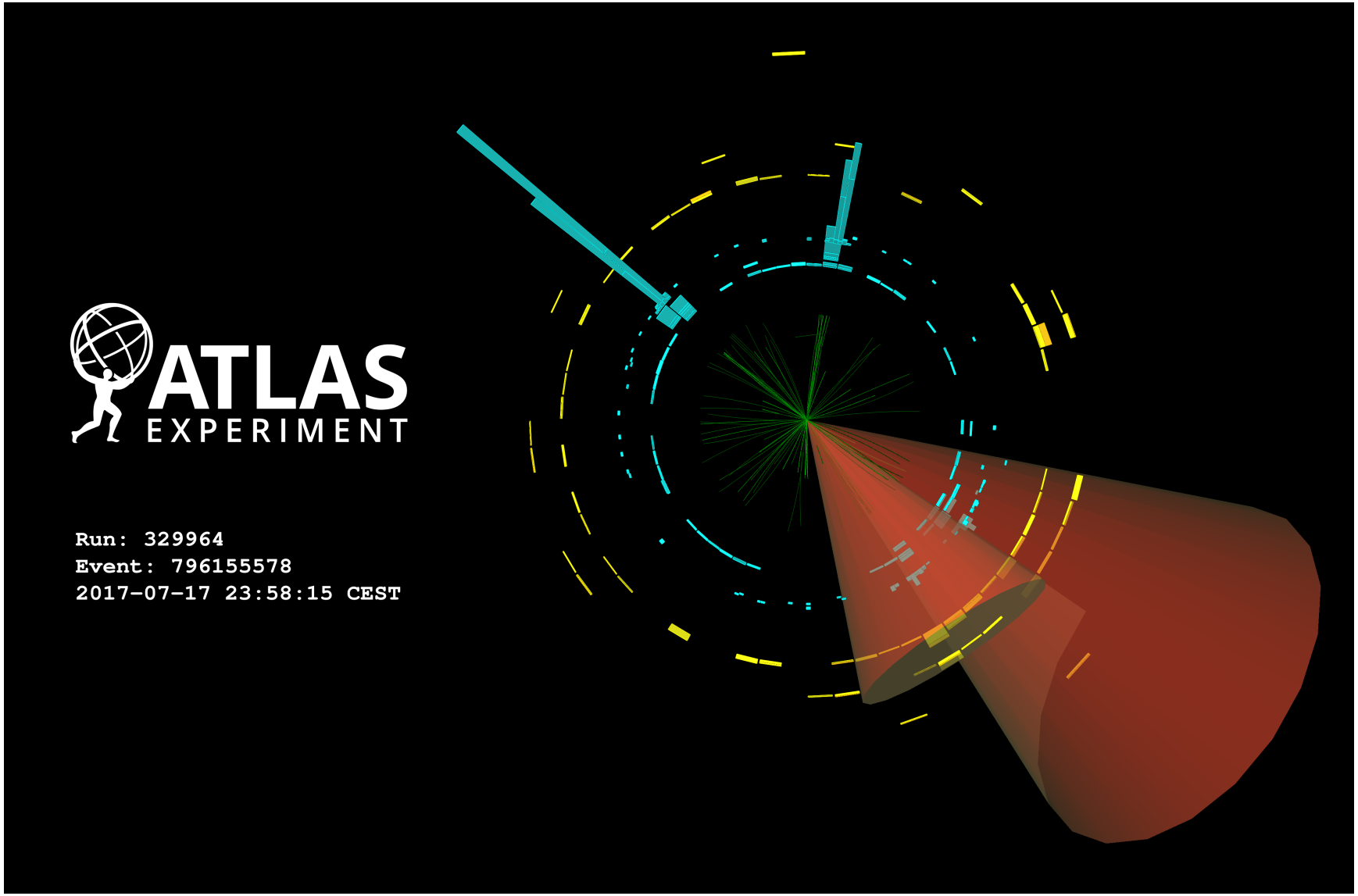
ATLAS
EXPERIMENT
Run: 329964
Event: 796155578
2017-07-17 23:58:15 CEST

HH production

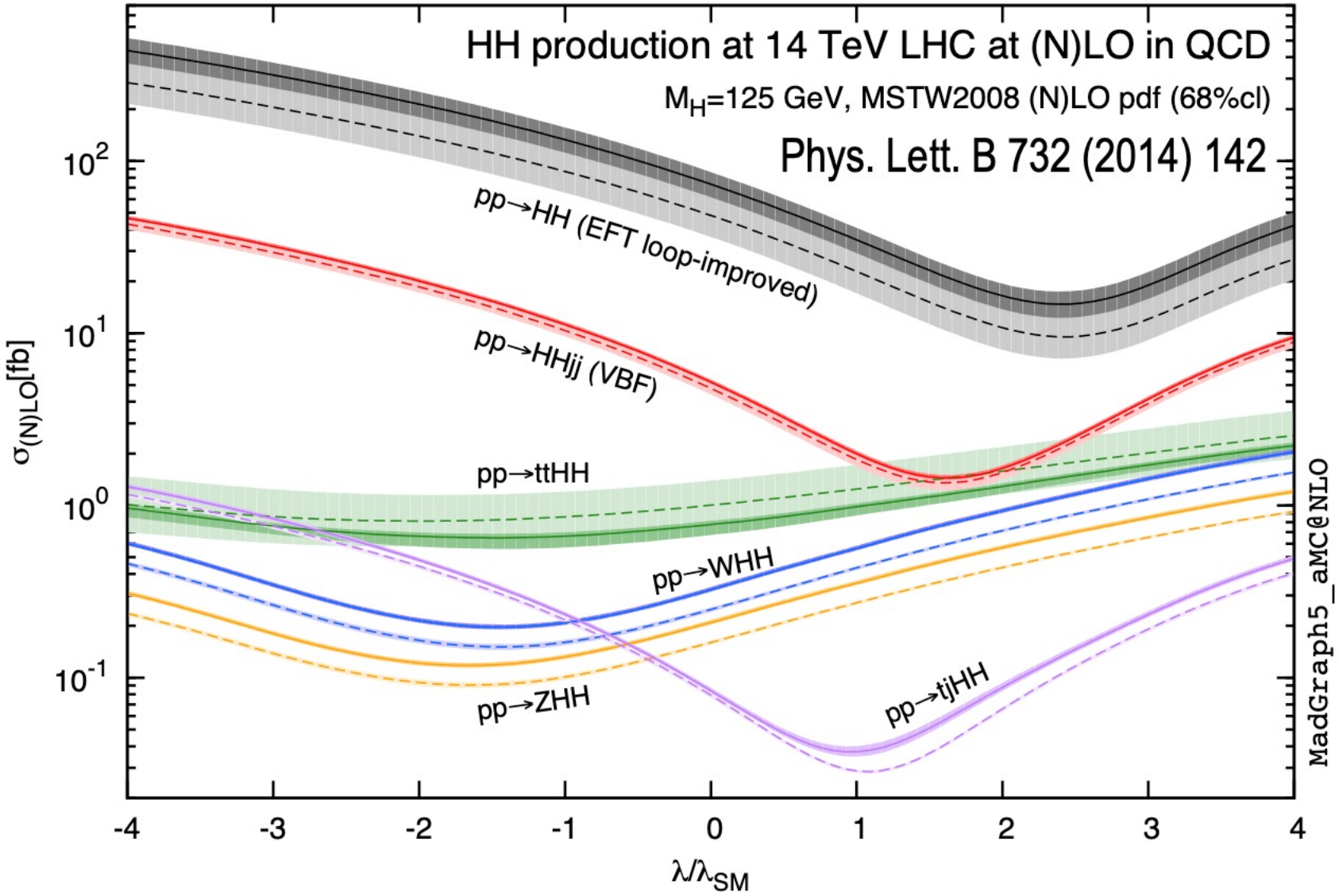

$HH \rightarrow b\bar{b}\gamma\gamma$ analysis in a nutshell

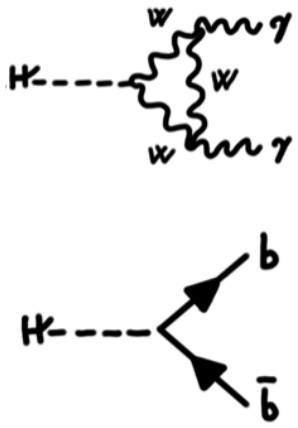

Object selection

Event categorization

MVA approach

4 categories for non-resonant analysis

1 category per m_X for resonant analysis

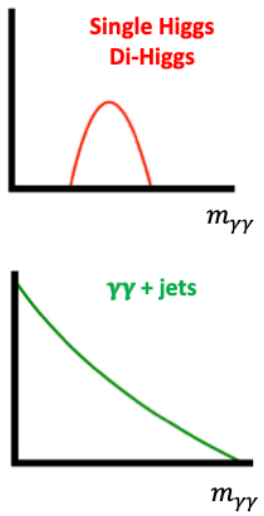

Modelling of discriminant variable

Simultaneous likelihood fit to all categories

SM σ limits and
σ vs k_λ
for non resonant analysis

σ vs m_X
for resonant analysis

Statistically limited with the current dataset

Background Samples

Table 1: Summary of single Higgs boson background samples, split by production modes, and continuum background samples. The generator used in the simulation, the PDF set, and tuned parameters (tune) are also provided.

Process	Generator	PDF set	Showering	Tune
ggF	NNLOPS [65–67] [68, 69]	PDFLHC [42]	Pythia 8.2 [70]	AZNLO [71]
VBF	Powheg Box v2 [39, 66, 72–78]	PDFLHC	Pythia 8.2	AZNLO
WH	Powheg Box v2	PDFLHC	Pythia 8.2	AZNLO
$qq \to ZH$	Powheg Box v2	PDFLHC	Pythia 8.2	AZNLO
$gg \to ZH$	Powheg Box v2	PDFLHC	Pythia 8.2	AZNLO
$t\bar{t}H$	Powheg Box v2 [73–75, 78, 79]	`NNPDF3.0nlo` [80]	Pythia 8.2	A14 [81]
bbH	Powheg Box v2	`NNPDF3.0nlo`	Pythia 8.2	A14
$tHqj$	MadGraph5_aMC@NLO	`NNPDF3.0nlo`	Pythia 8.2	A14
tHW	MadGraph5_aMC@NLO	`NNPDF3.0nlo`	Pythia 8.2	A14
$\gamma\gamma$+jets	Sherpa v2.2.4 [56]	`NNPDF3.0nnlo`	Sherpa v2.2.4	–
$t\bar{t}\gamma\gamma$	MadGraph5_aMC@NLO	`NNPDF2.3lo`	Pythia 8.2	–

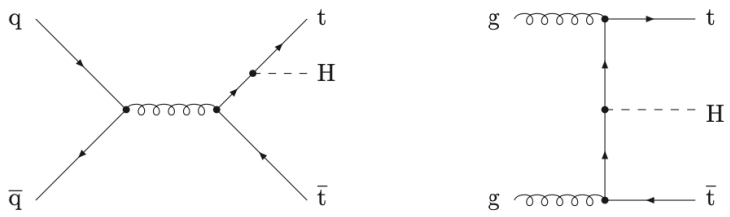

Fig. 12: Examples of LO Feynman diagrams for the partonic processes $q\bar{q}, gg \to t\bar{t}H$.

Event preselection

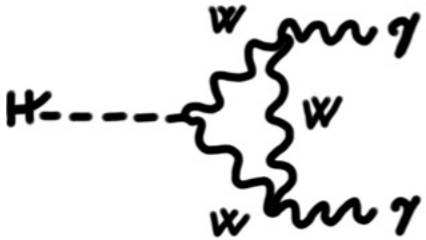

- Photon **identification** (Tight WP)
- Calorimeter- and track-based **isolation** within a cone of $\Delta R = 0.2$

  $E_T^{\text{iso}} < 0.065 \cdot E_T$ and $p_T^{\text{iso}} < 0.05 \cdot E_T$
- $105 < \boldsymbol{m_{\gamma\gamma}} < 160\ GeV$
- $p_T^{\gamma 1}/m_{\gamma\gamma} > 0.35,\ p_T^{\gamma 2}/m_{\gamma\gamma} > 0.25$

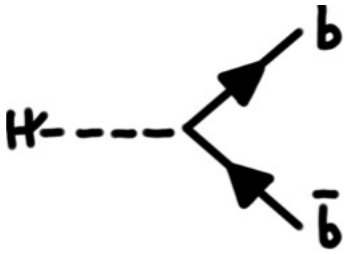

- **DL1r b-tagging** (a deep-learning neural network)

  WP: 77% efficiency
- **Energy correction**
  - **muon-in-jet** correction: muons from semileptonic b-hadron decays
  - **$\boldsymbol{p_T}$-reco** correction: p_T loss due to neutrinos and objects outside of the jet cone

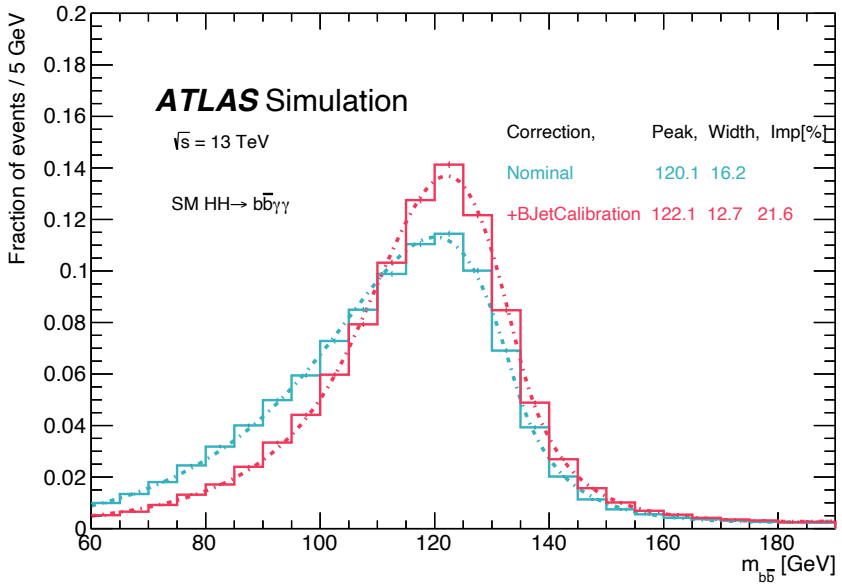

m_{bb} resolution improved by about 22%

Non-resonant BDT variables

Table 2: Variables used in the BDT for the non-resonant analysis. The b-tag status identifies the highest fixed b-tag working point (60%, 70%, 77%) that the jet passes. All vectors in the event are rotated so that the leading photon ϕ is equal to zero.

Variable	Definition
Photon-related kinematic variables	
$p_T/m_{\gamma\gamma}$	Transverse momentum of the two photons scaled by their invariant mass $m_{\gamma\gamma}$
η and ϕ	Pseudo-rapidity and azimuthal angle of the leading and sub-leading photon
Jet-related kinematic variables	
b-tag status	Highest fixed b-tag working point that the jet passes
p_T, η and ϕ	Transverse momentum, pseudo-rapidity and azimuthal angle of the two jets with the highest b-tagging score
$p_T^{b\bar{b}}$, $\eta_{b\bar{b}}$ and $\phi_{b\bar{b}}$	Transverse momentum, pseudo-rapidity and azimuthal angle of b-tagged jets system
★ $m_{b\bar{b}}$	Invariant mass built with the two jets with the highest b-tagging score
★ H_T	Scalar sum of the p_T of the jets in the event
Single topness	For the definition, see Eq. (1)
Missing transverse momentum-related variables	
E_T^{miss} and ϕ^{miss}	Missing transverse momentum and its azimuthal angle

$$\chi_{Wt} = \min\sqrt{\left(\frac{m_{j_1 j_2} - m_W}{m_W}\right)^2 + \left(\frac{m_{j_1 j_2 j_3} - m_t}{m_t}\right)^2},$$

Non-resonant Categorization

$$Z = \sqrt{2 * [(s+b) * \log(1 + s/b) - s]}$$

Low mass region

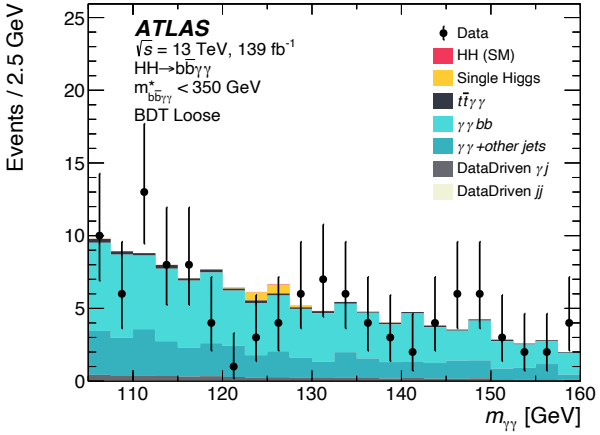

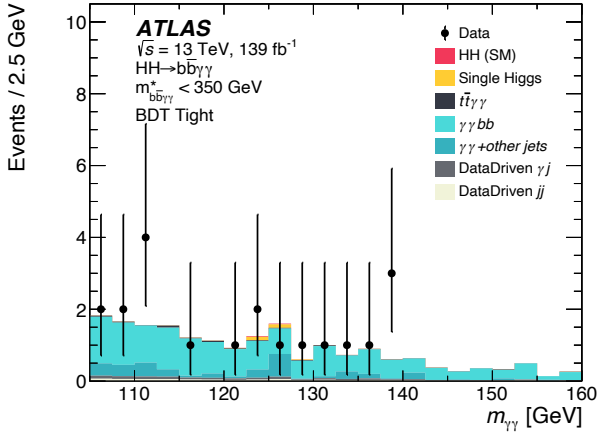

High mass region

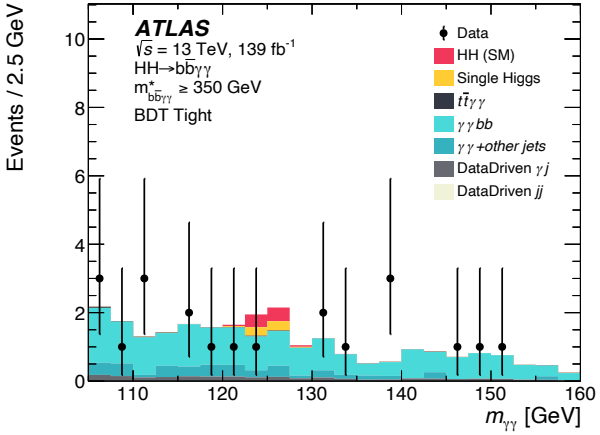

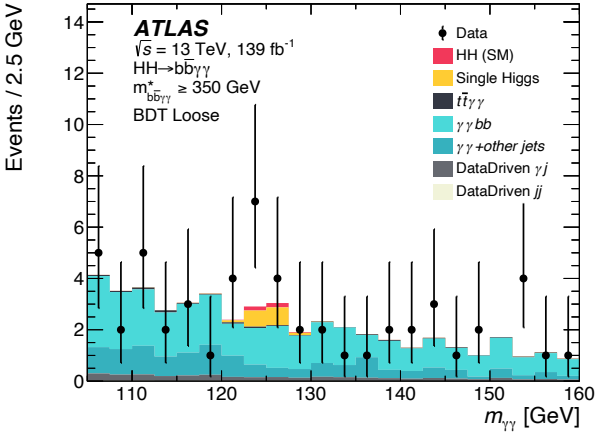

Resonant BDT variables

Table 4: Variables used in the BDT for the resonant analysis. For variables depending on b-tagged jets, only jets b-tagged using the 77% working point are considered as described in Section 4.1.

Variable	Definition
Photon-related kinematic variables	
$p_{\mathrm{T}}^{\gamma\gamma}$, $y^{\gamma\gamma}$	Transverse momentum and rapidity of the di-photon system
$\Delta\phi_{\gamma\gamma}$ and $\Delta R_{\gamma\gamma}$	Azimuthal angular distance and ΔR between the two photons
Jet-related kinematic variables	
$m_{b\bar{b}}$, $p_{\mathrm{T}}^{b\bar{b}}$ and $y_{b\bar{b}}$	Invariant mass, transverse momentum and rapidity of the b-tagged jets system
$\Delta\phi_{b\bar{b}}$ and $\Delta R_{b\bar{b}}$	Azimuthal angular distance and ΔR between the two b-tagged jets
N_{jets} and $N_{b-\mathrm{jets}}$	Number of jets and number of b-tagged jets
H_{T}	Scalar sum of the p_{T} of the jets in the event
Photons and jets-related kinematic variables	
$m_{b\bar{b}\gamma\gamma}$	Invariant mass built with the di-photon and b-tagged jets system
$\Delta y_{\gamma\gamma,b\bar{b}}$, $\Delta\phi_{\gamma\gamma,b\bar{b}}$ and $\Delta R_{\gamma\gamma,b\bar{b}}$	Distance in rapidity, azimuthal angle and ΔR between the di-photon and the b-tagged jets system

$$\mathrm{BDT}_{\mathrm{tot}} = \frac{1}{\sqrt{C_1^2 + C_2^2}} \sqrt{C_1^2 \left(\frac{\mathrm{BDT}_{\gamma\gamma} + 1}{2}\right)^2 + C_2^2 \left(\frac{\mathrm{BDT}_{\mathrm{Single}H} + 1}{2}\right)^2}$$

- **2-stage optimization**
  1. Maximize significance for each resonance
     - Different coefficients and BDT scores
  2. Select coefficients providing a significance within 5% from the maximum value, for each resonance
     - A common C_1 = 0.65 coefficient is found, individual BDT cuts are used

Signal modeling - DSCB

A Gaussian core + asymmetric power law tails

$$f_{\mathrm{DSCB}}(m_{\gamma\gamma}) = N \times \begin{cases} e^{-t^2/2} & \text{if } -\alpha_{low} \le t \le \alpha_{high} \\ \dfrac{e^{-\frac{1}{2}\alpha_{low}^2}}{\left[\frac{1}{R_{low}}\left(R_{low} - \alpha_{low} - t\right)\right]^{n_{low}}} & \text{if } t < -\alpha_{low} \\ \dfrac{e^{-\frac{1}{2}\alpha_{high}^2}}{\left[\frac{1}{R_{high}}\left(R_{high} - \alpha_{high} + t\right)\right]^{n_{high}}} & \text{if } t > \alpha_{high} \end{cases}$$

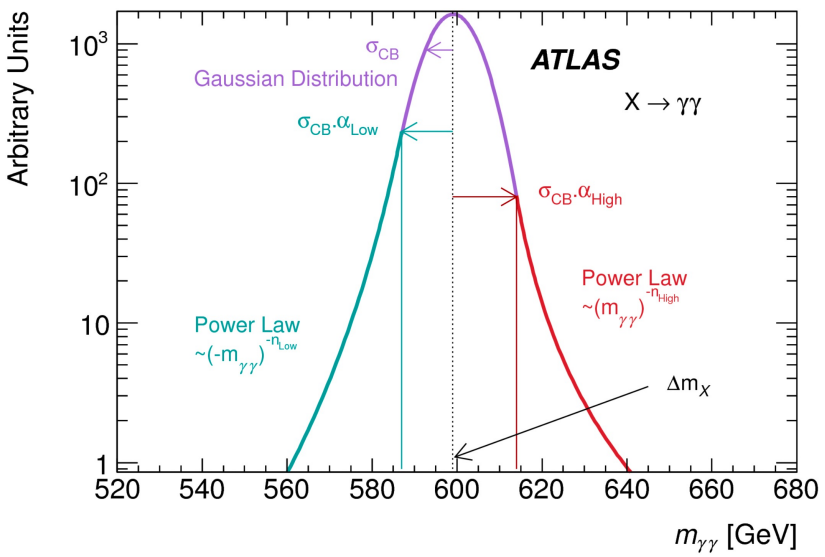

where N is a normalization factor and the six parameters are

- μ_{CB} and σ_{CB} describe the mean and the width of the Gaussian core, which are combined in $t = \left(m_{\gamma\gamma} - \mu_{\mathrm{CB}}\right)/\sigma_{\mathrm{CB}}$;
- α_{low} and α_{high} are the positions of the transitions with respect to μ_{CB} from the Gaussian core to power-law tails, in unit of σ_{CB}, on the low and high mass sides respectively;
- n_{low} and n_{high} are the exponents of the low and high mass tails. With the α's, they define $R_{low} = \frac{n_{low}}{\alpha_{low}}$ and R_{high} similarly.

non-Gaussian tails can arise from experimental effects, such as photon energy mismeasurements.

One of the main benefits is the ability to describe the effects of systematic uncertainties in its shape with extra parameters

Diphoton background decomposition

- Reconstructed $\gamma\gamma$ events is mainly composed of $\gamma\gamma$, γ-jets and jet-jet events, where **the jet(s) fake(s) a real photon.**
- The 2x2D sideband method is developed using the discriminating power of **photon identification and isolation criteria.**
- The event yields in the signal region and the 15 sidebands can be expressed as **functions** of the photon efficiencies, jet fake rates and correlation coefficients.

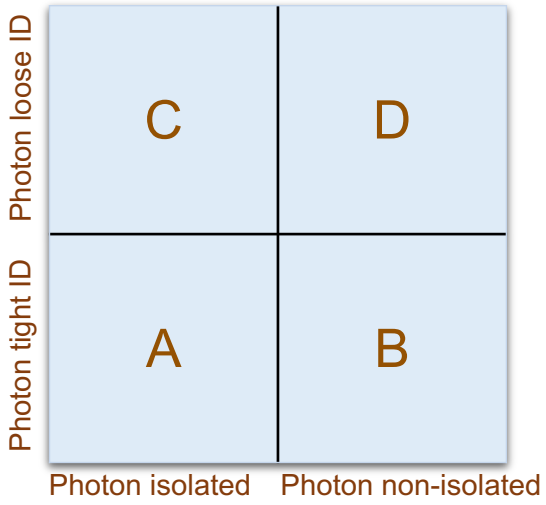

Leading object

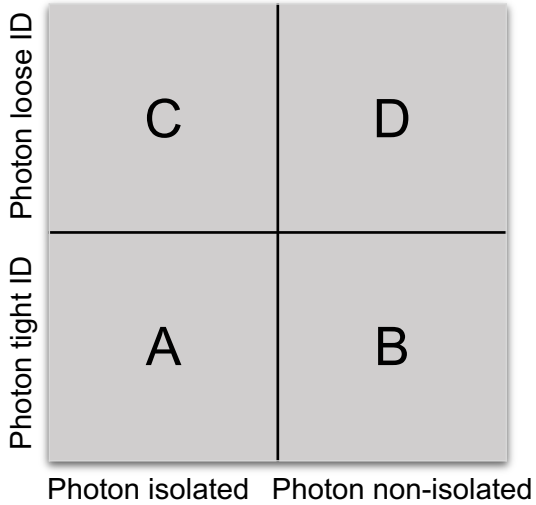

Sub-leading object

CC	CD	DC	DD
CA	CB	DA	DB
AC	AD	BC	BD
AA	AB	BA	BB

Reference

Suffers from **low statistics**, not used in constructing the background templates for the spurious signal procedure.

Spurious signal

Spurious signal: a bias estimated from a **signal + background** fit to a **background-only** MC template.

$$N_{sp} = \max_{121<m_H<129\ GeV} |N_s(m_H)|$$

➢ **Selection criteria:**

- N_{sp} < 20% of the data's statistical uncertainty + 2 × the MC background template statistical uncertainty
- must satisfy a simple χ^2 requirement in a background-only fit to the MC template: $p - value(\chi^2) > 1\%$

- **The least number of parameters** is preferred.
- The **smaller systematic uncertainty** (spurious signal) is preferred.

Wald tests show that the data do not prefer a higher degree functional form with respect to the exponential form.

Systematic uncertainties

In general the analysis is almost completely **statistically dominated** with the Run 2 dataset

		Relative impact of the systematic uncertainties [%]	
Source	Type	Nonresonant analysis HH	Resonant analysis $m_X = 300$ GeV
Experimental			
Photon energy resolution	Norm. + Shape	0.4	0.6
Jet energy scale and resolution	Normalization	< 0.2	0.3
Flavor tagging	Normalization	< 0.2	0.2
Theoretical			
Factorization and renormalization scale	Normalization	0.3	< 0.2
Parton showering model	Norm. + Shape	0.6	2.6
Heavy-flavor content	Normalization	0.3	< 0.2
$\mathcal{B}(H \to \gamma\gamma, b\bar{b})$	Normalization	0.2	< 0.2
Spurious signal	Normalization	3.0	3.3

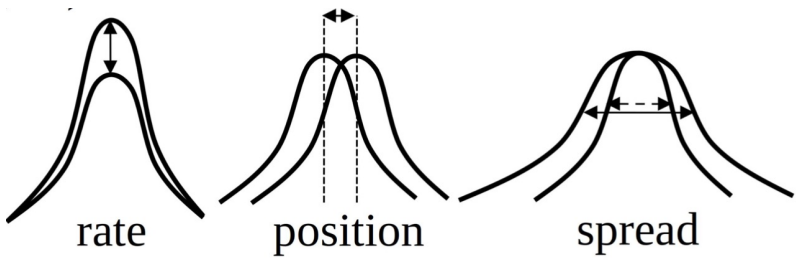

Statistical framework

- The results of the analysis are obtained from a **maximum-likelihood fit** of the $m\gamma\gamma$ distribution.

Likelihood

$$\mathcal{L} = \prod_{c} \left(\mathrm{Pois}(n_c | \boxed{N_c(\boldsymbol{\theta})}) \cdot \prod_{i=1}^{n_c} \boxed{f_c(m^i_{\gamma\gamma}, \boldsymbol{\theta})} \cdot G(\boldsymbol{\theta}) \right)$$

Event parameterization

$$\boxed{N_c(\boldsymbol{\theta})} = \mu \cdot N_{HH,\mathrm{c}}(\boldsymbol{\theta}^{\mathrm{yield}}_{HH}) + N^{\mathrm{res}}_{\mathrm{bkg,c}}(\boldsymbol{\theta}^{\mathrm{yield}}_{\mathrm{res}}) + N_{\mathrm{SS,c}} \cdot \boldsymbol{\theta}^{\mathrm{SS,c}} + N^{\mathrm{non-res}}_{\mathrm{bkg,c}}$$

Model PDF

$$\boxed{f_c(m_{\gamma\gamma}, \boldsymbol{\theta})} = [\mu \cdot N_{HH,\mathrm{c}}(\boldsymbol{\theta}^{\mathrm{yield}}_{HH}) \cdot f_{HH,\mathrm{c}}(m_{\gamma\gamma}, \boldsymbol{\theta}^{\mathrm{shape}}_{HH}) + N^{\mathrm{res}}_{\mathrm{bkg,c}}(\boldsymbol{\theta}^{\mathrm{yield}}_{\mathrm{res}}) \cdot f^{\mathrm{res}}_{\mathrm{bkg,c}}(m_{\gamma\gamma}, \boldsymbol{\theta}^{\mathrm{shape}}_{\mathrm{res}})$$
$$+ N_{\mathrm{SS,c}} \cdot \boldsymbol{\theta}^{\mathrm{SS,c}}_{HH} \cdot f_{HH,\mathrm{c}}(m_{\gamma\gamma}, \boldsymbol{\theta}^{\mathrm{shape}}_{HH}) + N^{\mathrm{non-res}}_{\mathrm{bkg,c}} \cdot f^{\mathrm{non-res}}_{\mathrm{bkg,c}}(m_{\gamma\gamma}, \boldsymbol{\theta}^{\mathrm{shape}}_{\mathrm{non-res}})] / N_c(\boldsymbol{\theta}^{\mathrm{yield}}_{\mathrm{non-res}}),$$

Statistical framework

- The measurement of the parameter of interest is carried out using a statistical test based on the **profile likelihood ratio**

the profile likelihood ratio

$$\Lambda(\mu) = \frac{\mathcal{L}(\mu, \hat{\hat{\boldsymbol{\theta}}}(\mu))}{\mathcal{L}(\hat{\mu}, \hat{\boldsymbol{\theta}})}$$

the profile-likelihood-ratio-based test statistic

$$\tilde{q}_\mu = \begin{cases} -2\ln\frac{\Lambda(\mu, \hat{\hat{\boldsymbol{\theta}}}(\mu))}{\Lambda(0, \hat{\hat{\boldsymbol{\theta}}}(0))} & \hat{\mu} < 0, \\ -2\ln\frac{\Lambda(\mu, \hat{\hat{\boldsymbol{\theta}}}(\mu))}{\Lambda(\hat{\mu}, \hat{\boldsymbol{\theta}}(\mu))} & 0 \le \hat{\mu} \le \mu, \\ 0 & \hat{\mu} > \mu. \end{cases}$$

κ_λ reweighting for ggF HH samples

Common HH procedure. The method derives the **scale factors as a function of κ_λ** in **bins of m_{HH}** by performing a **linear combination** of samples generated at $\kappa_\lambda = 0, 1, 20$.

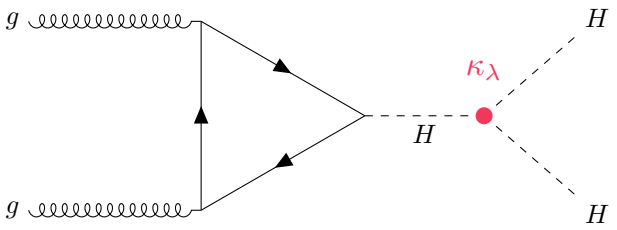

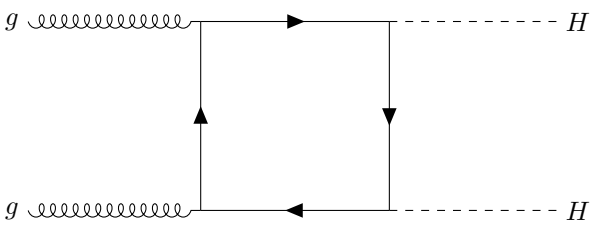

$$\mathcal{A}(\kappa_t, \kappa_\lambda) = \kappa_t^2 \mathcal{A}_1 + \kappa_t \kappa_\lambda \mathcal{A}_2$$

$$\sigma_{\mathrm{ggF}}(pp \to HH) \propto \int \kappa_t^4 \left[|\mathcal{A}_1|^2 + 2\left(\frac{\kappa_\lambda}{\kappa_t}\right) \Re(\mathcal{A}_1^* \mathcal{A}_2) + \left(\frac{\kappa_\lambda}{\kappa_t}\right)^2 |\mathcal{A}_2|^2 \right]$$

$$\sigma(\kappa_t = 1, \kappa_\lambda = 0) \sim |\mathcal{A}_1|^2$$

$$\sigma(\kappa_t = 1, \kappa_\lambda = 1) \sim |\mathcal{A}_1|^2 + 2\Re \mathcal{A}_1^* \mathcal{A}_2 + |\mathcal{A}_2|^2$$

$$\sigma(\kappa_t = 1, \kappa_\lambda = 20) \sim |\mathcal{A}_1|^2 + 2 \cdot 20 \Re \mathcal{A}_1^* \mathcal{A}_2 + 20^2 |\mathcal{A}_2|^2$$

$$\sigma(\kappa_t, \kappa_\lambda) \sim \kappa_t^2 \left[\left(\kappa_t^2 + \frac{\kappa_\lambda^2}{20} - \frac{399}{380} \kappa_\lambda \kappa_t \right) |S(1,0)|^2 + \left(\frac{40}{38} \kappa_\lambda \kappa_t - \frac{2}{38} \kappa_\lambda^2 \right) |S(1,1)|^2 + \left(\frac{\kappa_\lambda^2 - \kappa_\lambda \kappa_t}{380} \right) |S(1,20)|^2 \right]$$

$$d\sigma/dm_{HH} = A(m_{HH}) + B(m_{HH})\kappa_\lambda + C(m_{HH})\kappa_\lambda^2$$

HH summary

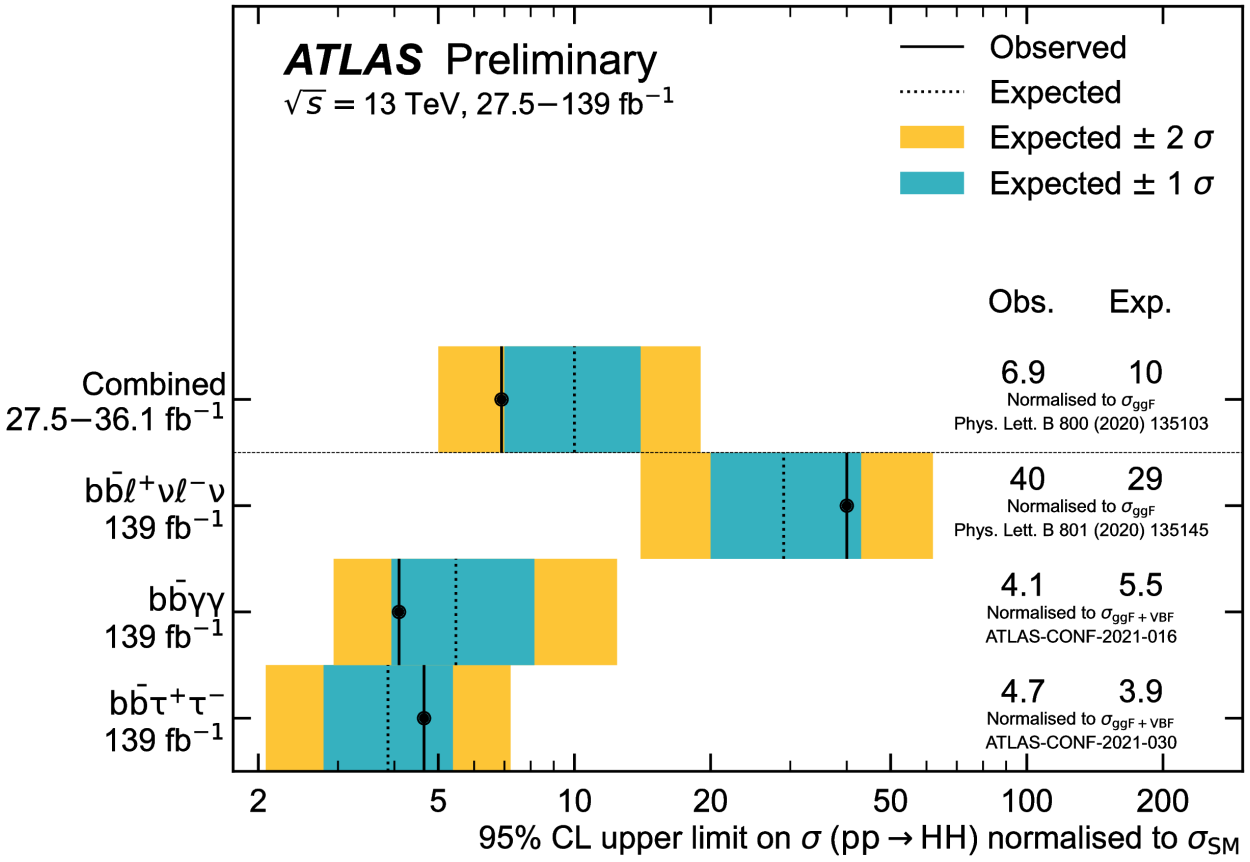

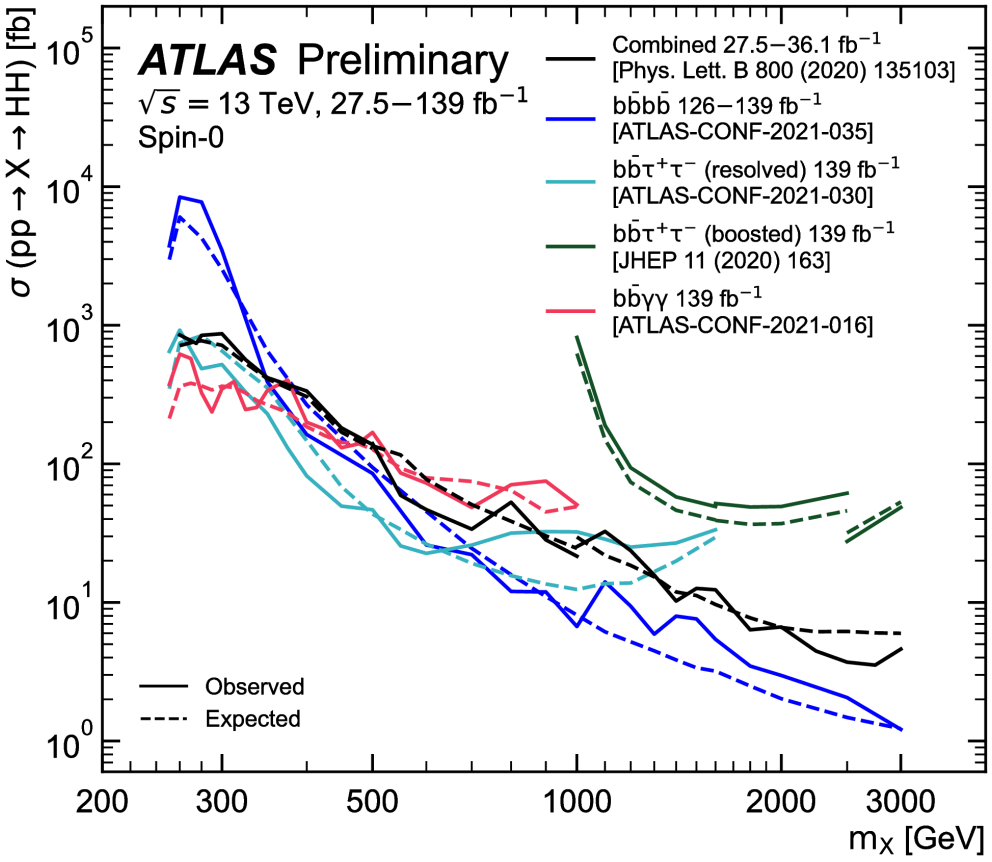

good sensitivity at low resonant masses

ttgammagamma

```
import model sm-no_b_mass
define p = g u c d s b u~ c~ d~ s~ b~
define l+ = e+ mu+ ta+
define vl = ve vm vt
define uc~ = u~ c~
define ds = d s
define l- = e- mu- ta-
define vl~ = ve~ vm~ vt~
define uc = u c
define ds~ = d~ s~
generate p p > t t~ > l+ vl b ds uc~ b~ a a QCD=2 QED=6 \n
add process p p > t t~ > uc ds~ b l- vl~ b~ a a QCD=2 QED=6 \n
add process p p > t t~ > l+ vl b l- vl~ b~ a a QCD=2 QED=6 """
```